# Supplementary Information

## A facile way to prepare nanoporous $PbI_2$ films and their application in fast conversion into $CH_3NH_3PbI_3$

Huifeng Zheng,[a] Weiqi Wang,[a] Songwang Yang,[b] Yangqiao Liu,*[a] and Jing Sun*[a]

[a] State Key Laboratory of High Performance Ceramics and Superfine Microstructure, Shanghai Institute of Ceramics, Chinese Academy of Sciences, 1295 Dingxi Road, Shanghai 200050, P. R.China.

[b] CAS Key Laboratory of Materials for Energy Conversion, Shanghai Institute of Ceramics, Chinese Academy of Sciences, 588 Heshuo Road, Shanghai 201899, P. R. China

*To whom correspondence should be addressed:

E-mail: yqliu@mail.sic.ac.cn

E-mail: jingsun@mail.sic.ac.cn

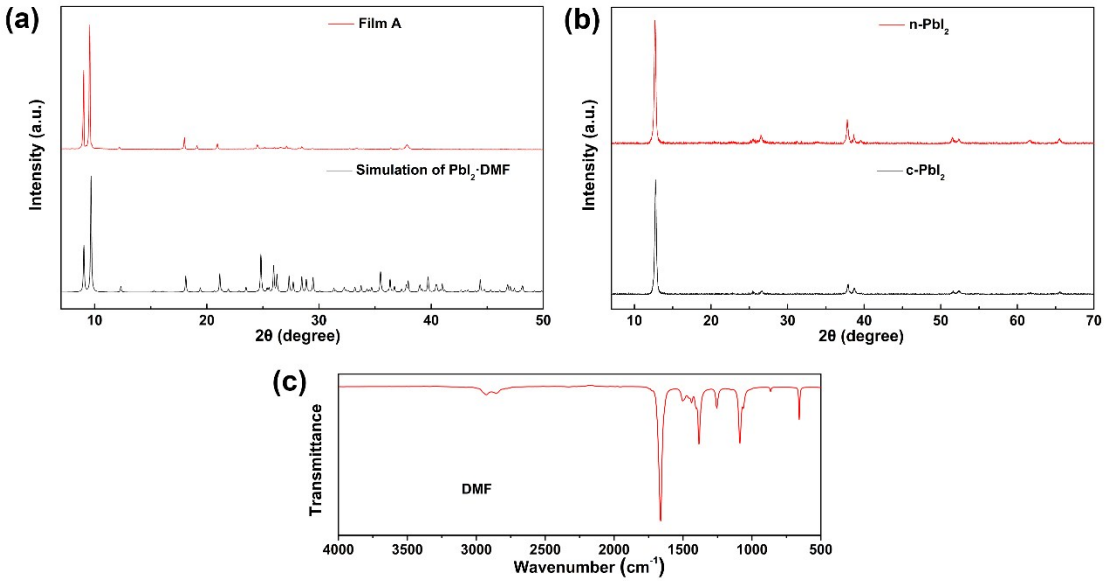


Fig. S1. The comparison of XRD spectra between (a) Film A and the simulation pattern of $PbI_2$·DMF; (b) n-$PbI_2$ film and c-$PbI_2$ film. (c) FTIR spectrum of DMF. The simulation is conducted by the software Mercury 3.6, based on the crystallographic data (CCDC-982210) from Cambridge Crystallographic Data Centre (CCDC).

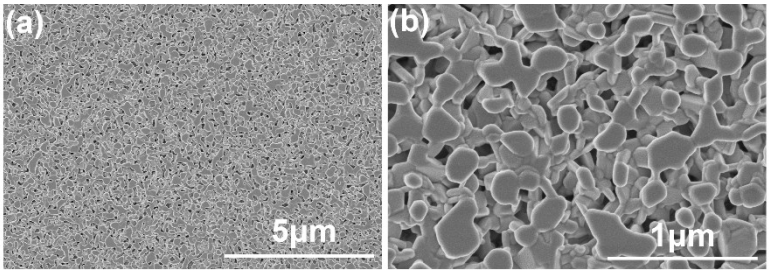


Fig. S2. (a) Low magnification and (b) high magnification SEM images of n-$PbI_2$ with toluene as the extraction solvent for SSE process.

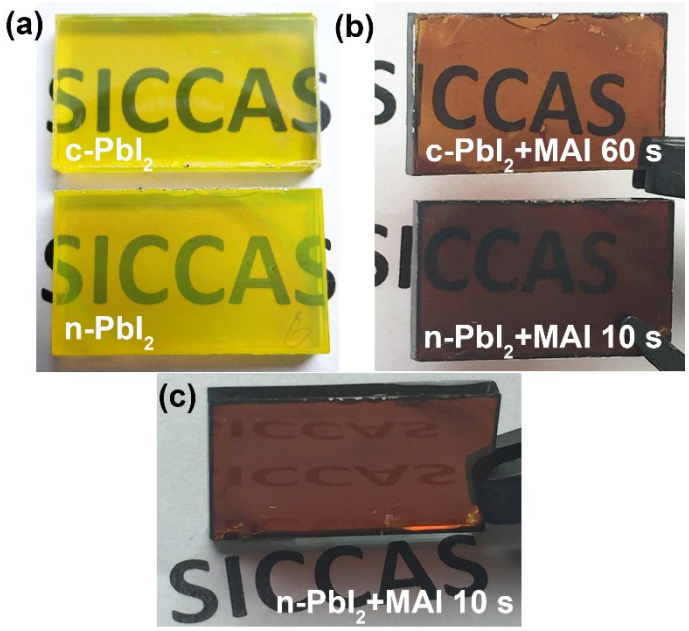


Fig. S3. Photographs of (a) c-$PbI_2$ and n-$PbI_2$ films, (b) perovskite films based on c-$PbI_2$ film (dipped in MAI solution for 60 s) and n-$PbI_2$ film (dipped in MAI solution for 10 s), (c) the same perovskite film in (b) based on n-$PbI_2$ film shows high reflectivity.

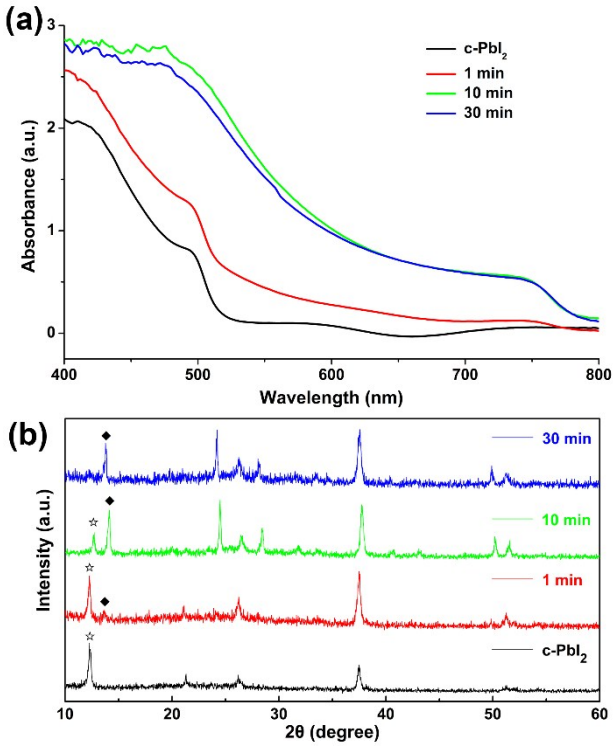


Fig. S4. Effect of dipping time in MAI solution (10 mg/ml, in IPA) on the evolution of (a) UV-vis absorption spectra and (b) XRD spectra of perovskite films based on c-$PbI_2$ films. Some peaks are labelled : (☆)- (001) of $PbI_2$, (◆) - (110) of $MAPbI_3$ perovskite.

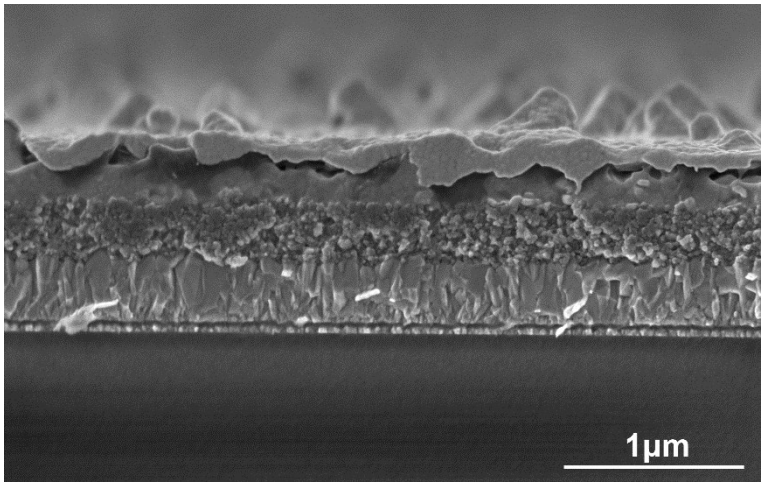


Fig. S5. Cross-sectional SEM image of perovskite solar cell with bilayer structure. The perovskite layer was prepared by dipping c-$PbI_2$ film into MAI solution (10 mg/ml, in IPA) for 5min. The perovskite overlayer is too rough to be totally covered by P3HT layer, resulting from the abnormal crystal growth when dipping too long. As a result, the Ag layer is not flat as well, contacting with perovskite layer certainly.

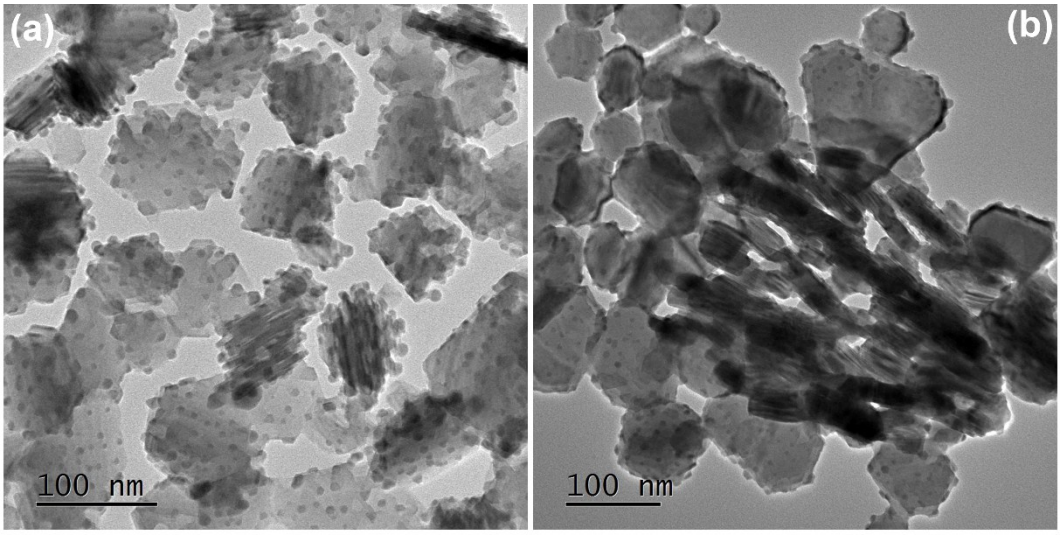


Fig. S6. TEM images of $PbI_2$ crystallites scratched from (a) c-$PbI_2$ and (b) n-$PbI_2$ films. The crystallites from both films are nanoplate, and the nanoplates of n-$PbI_2$ are smaller than that of c-$PbI_2$. Those tiny crystallites around 10 nm originated from the decomposition and regrowth of the larger $PbI_2$ nanoplates under the electron beam irradiation. The TEM images were obtained as quickly as we could, though some tiny crystallites generated, the original morphology were obtained.

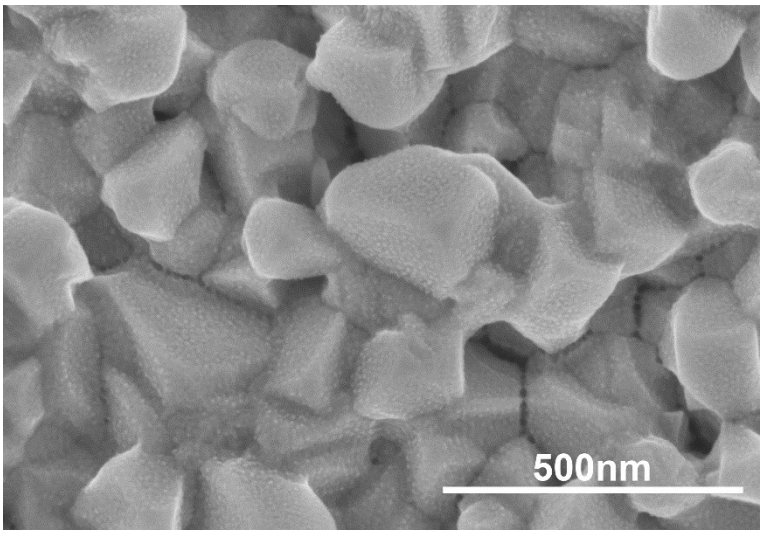


Fig. S7. High magnification SEM image of n-$PbI_2$ based perovskite film, which was prepared by dipping n-$PbI_2$ film into MAI solution (10 mg/ml, in IPA) for 40 s. From the image, we can see that the perovskite layer is pinhole free except some cracks at the grain boundary.

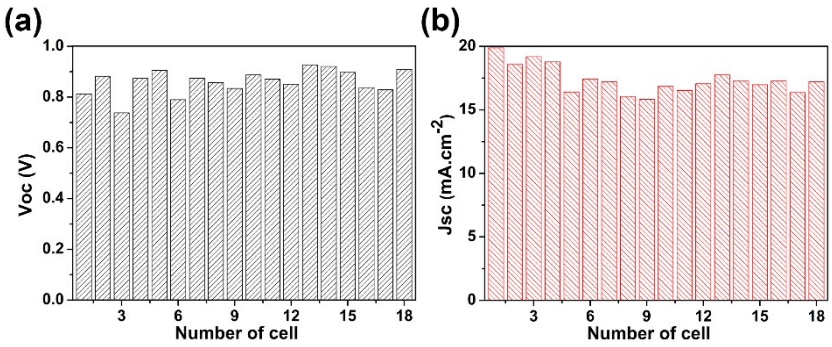


Fig. S8. Histogram of (a) open-circuit voltage ($V_{oc}$) and (b) short-circuit current density ($J_{sc}$) of 18 cells.

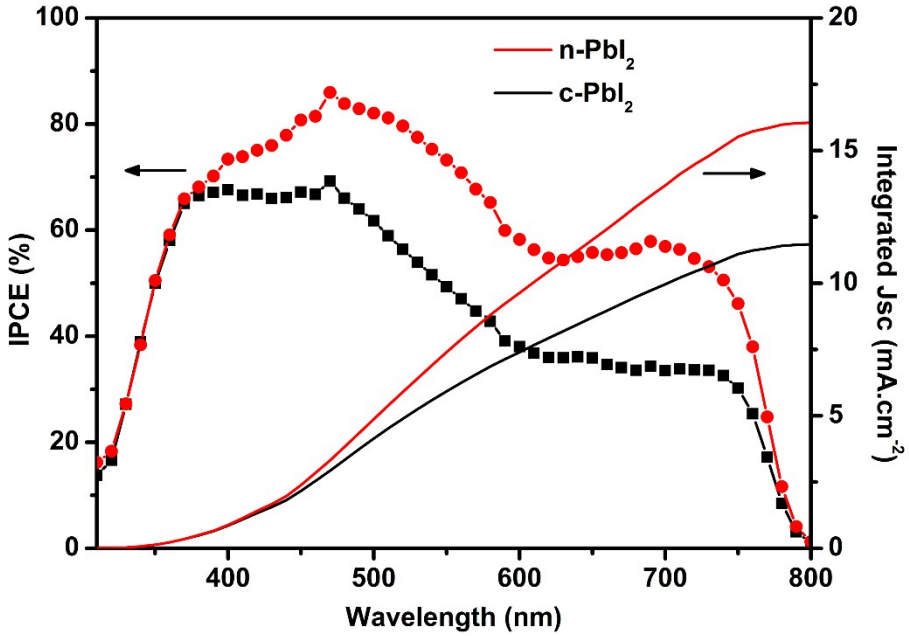


Fig. S9. IPCE spectra and integrated $J_{sc}$ of n-$PbI_2$ and c-$PbI_2$ based perovskite solar cells. The integrated $J_{sc}$ for n-$PbI_2$ and c-$PbI_2$ based solar cells are 16.1 mA.cm$^{-2}$ and 11.5 mA.cm$^{-2}$, respectively. Both of them agree well with the measured photocurrent density from the J-V curves, which are 16.9 mA.cm$^{-2}$ and 12.8 mA.cm$^{-2}$ for n-$PbI_2$ and c-$PbI_2$ based solar cells, respectively.